Contents lists available at ScienceDirect

Arabian Journal of Chemistry

journal homepage: www.ksu.edu.sa

Original article

Enhancing the quality and antioxidant capacity of phycocyanin extracted from *Spirulina platensis* PCC 7345: A quality-by-design approach

Additiya Paramanya [a], Abeeb Oyesiji Abiodun [b], Mohammad Shamsul Ola [c,*], Ahmad Ali [a,*]

[a] Department of Life Sciences, University of Mumbai, Mumbai 400098, India
[b] Department of Biological Sciences, Louisiana State University, Baton Rouge, LA 70802, USA
[c] Department of Biochemistry, College of Science, King Saud University, Riyadh 11451, Saudi Arabia

ARTICLE INFO

Keywords:
Antioxidant potential
Critical Quality Attributes (CQAs)
Phycocyanin
Quality by Design (QbD) approach
Target Product Profiles (TPPs)

ABSTRACT

Background and Objectives: Phycocyanin, a water-soluble blue pigment extracted from cyanobacteria, is used in various industries. Research has explored its health benefits like antioxidants and anti-inflammatory properties. However, challenges remain in extracting it efficiently and ensuring stability. This study employs a Quality by Design (QbD) approach to extract Phycocyanin from *Spirulina platensis* PCC 7345, focusing on Target Product Profiles (TPPs) and Critical Quality Attributes (CQAs). Phycocyanin concentration and purity are the primary CQAs, as they significantly impact product quality. The manuscript investigates the application of the Box-Behnken design to achieve consistentcy extraction of phycocyanin. **Methods:** Risk assessment via Ishikawa diagrams highlights influential factors. A Box Behnken design evaluates Phycocyanin concentration and purity across 15 formulations. Fourier transform infrared spectroscopy (FTIR) analysis affirms quality, sodium dodecyl sulphate–polyacrylamide gel electrophoresis (SDS-PAGE) validates protein structure, and gas chromatography provides additional insights into molecular composition. Antioxidant potential and enzyme inhibitory activities of the extracted Phycocyanin were analyzed. **Results:** Phycocyanin exhibits superior antioxidant potential, with half-maximal inhibitory concentration (IC_{50}) values for 2, 2-diphenyl-1-picrylhydrazyl (DPPH), 2, 2′-casino-bis (3-ethylbenzothiazoline-6-sulfonic acid) (ABTS), and Nitric Oxide Scavenging activity being 40.70 μg/ml, 23.25 μg/ml, and 17.74 μg/ml, respectively. The therapeutic potential of phycocyanin can be confirmed with its effectiveness in inhibition of α-Amylase and α-glucosidase enzymes in a concentration-dependent manner having IC_{50} values of 72.24 μg/ml and 82.45 μg/ml respectively. *Conclusion:* The QbD approach ensures quality Phycocyanin extraction. Its antioxidant and enzyme inhibitory properties indicate a promising role in diverse applications in health management.

1. Introduction

In recent years, the search for natural bioactive compounds with potential health benefits has gained significant momentum in food and pharmaceutical sciences. Spirulina, a blue-green microalga, has garnered considerable attention due to its rich content of bioactive molecules (Paramanya et al., 2023b). Phycobiliproteins are the light-harvesting complex found most commonly in Spirulina. They are further divided into four types based on their absorption wavelengths: phycocyanin (620–640 nm), allophycocyanin (650–660 nm), phycoerythrocyanin (550–575 nm), and phycoerythrin (500–575 nm) (Pagels et al., 2019). Phycocyanin is the most abundant protein found in cyanobacteria and is assumed to be responsible for the antioxidant properties of phycobiliprotein (Paramanya et al., 2023b). Phycocyanin has demonstrated a wide array of potential health-promoting properties, such as antioxidant, anti-inflammatory, and immunomodulatory effects, making it an appealing candidate for applications in nutraceuticals and functional foods (Fernandes et al., 2023). Extensive research has underscored its prowess in scavenging reactive oxygen species (ROS) and mitigating oxidative stress, a fundamental player in the realm of chronic diseases, including diabetes and its multifaceted complications (Martinez-Gonzalez et al., 2017).

Oxidative stress, a hallmark of various chronic diseases, including diabetes, results from the imbalance between harmful reactive oxygen species (ROS) production and the body's repair mechanisms (Pokhrel et al., 2022). Given its robust antioxidant potential, phycocyanin stands

* Corresponding authors.
E-mail addresses: mola@ksu.edu.sa (M. Shamsul Ola), ahmadali@mu.ac.in (A. Ali).

https://doi.org/10.1016/j.arabjc.2024.105653
Received 5 December 2023; Accepted 23 January 2024
Available online 26 January 2024

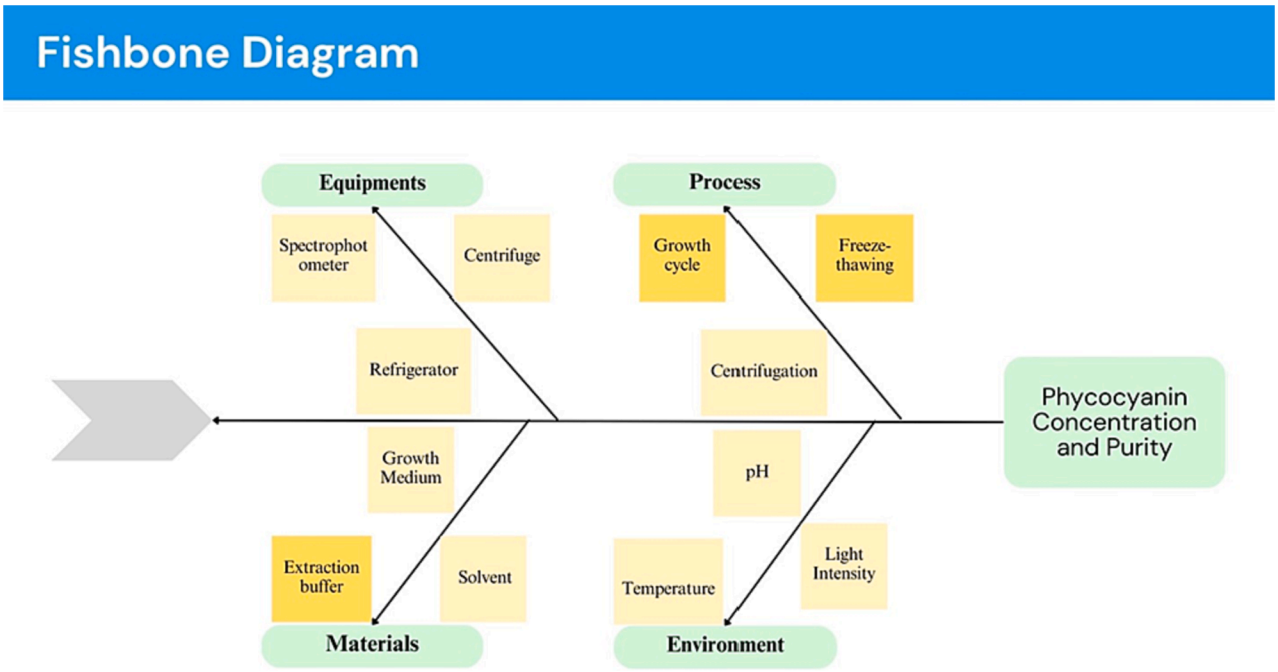

Fig. 1. Ishikawa fishbone diagram representing the factors that influence Phycocyanin Concentration and Purity. [The three factors selected for assessment have been highlighted in yellow.].

Table 1
Box Behnken Design for Extraction of Phycocyanin.

		Factor 1	Factor 2	Factor 3	Response 1	Response 2
Std	Run	A:Growth phase	B:Concentration of Buffer	C:Number of cycles	Phycocyanin Concentration	Phycocyanin Purity
		Days	M	Au	mg/ml	Au
9	1	9	0	2	0.0138	0.3112
10	2	9	1	2	0.02	0.259
3	3	3	1	3	0.043	0.202
12	4	9	1	4	0.1207	0.432
4	5	15	1	3	0.2812	0.6948
7	6	3	0.5	4	0.0338	0.17
13	7	9	0.5	3	0.102	0.3567
1	8	3	0	3	0.0608	0.2814
5	9	3	0.5	2	0.0121	0.32
15	10	9	0.5	3	0.1419	0.3306
6	11	15	0.5	2	0.0158	0.3644
14	12	9	0.5	3	0.09698	0.3615
8	13	15	0.5	4	0.1253	0.2833
2	14	15	0	3	0.0332	0.2454
11	15	9	0	4	0.0641	0.5116

Table 2
Model Summary Statistics for Response 1.

Source	Std. Dev.	R^2	Adjusted R^2	Predicted R^2	PRESS	
Linear	0.0598	0.4513	0.3016	−0.1046	0.0792	
2FI	0.0489	0.7332	0.5331	−0.1241	0.0806	
Quadratic	**0.0359**	**0.9104**	**0.7491**	**−0.2014**	**0.0862**	**Suggested**
Cubic	0.0246	0.9831	0.8818		*	Aliased

out as a promising candidate for mitigating oxidative stress in the context of diabetes, a condition often characterized by elevated oxidative stress levels (Paramanya and Ali, 2019). Phycocyanin exerts control over carbohydrate absorption by inhibiting amylase and glucosidase enzymes, resulting in a gradual increase in post-meal blood glucose levels. This measured response reduces oxidative stress associated with elevated glucose levels and reactive oxygen species production, making phycocyanin a promising candidate for diabetes management. Its multifaceted role in regulating blood sugar and mitigating oxidative stress offers new avenues for improving diabetes care (Poojari et al., 2022; Shrestha et al., 2021).

Phycocyanin's multifaceted attributes, primarily its antioxidant capabilities, position it as a versatile agent in managing diabetes. This versatility suggests ongoing research, product development, and the exploration of phycocyanin's role as a valuable natural compound to enhance health outcomes across different diseases (Poojari et al., 2022; Shrestha et al., 2021). This research aims to extract Phycocyanin from Spirulina and determine its antioxidant potential and capability to

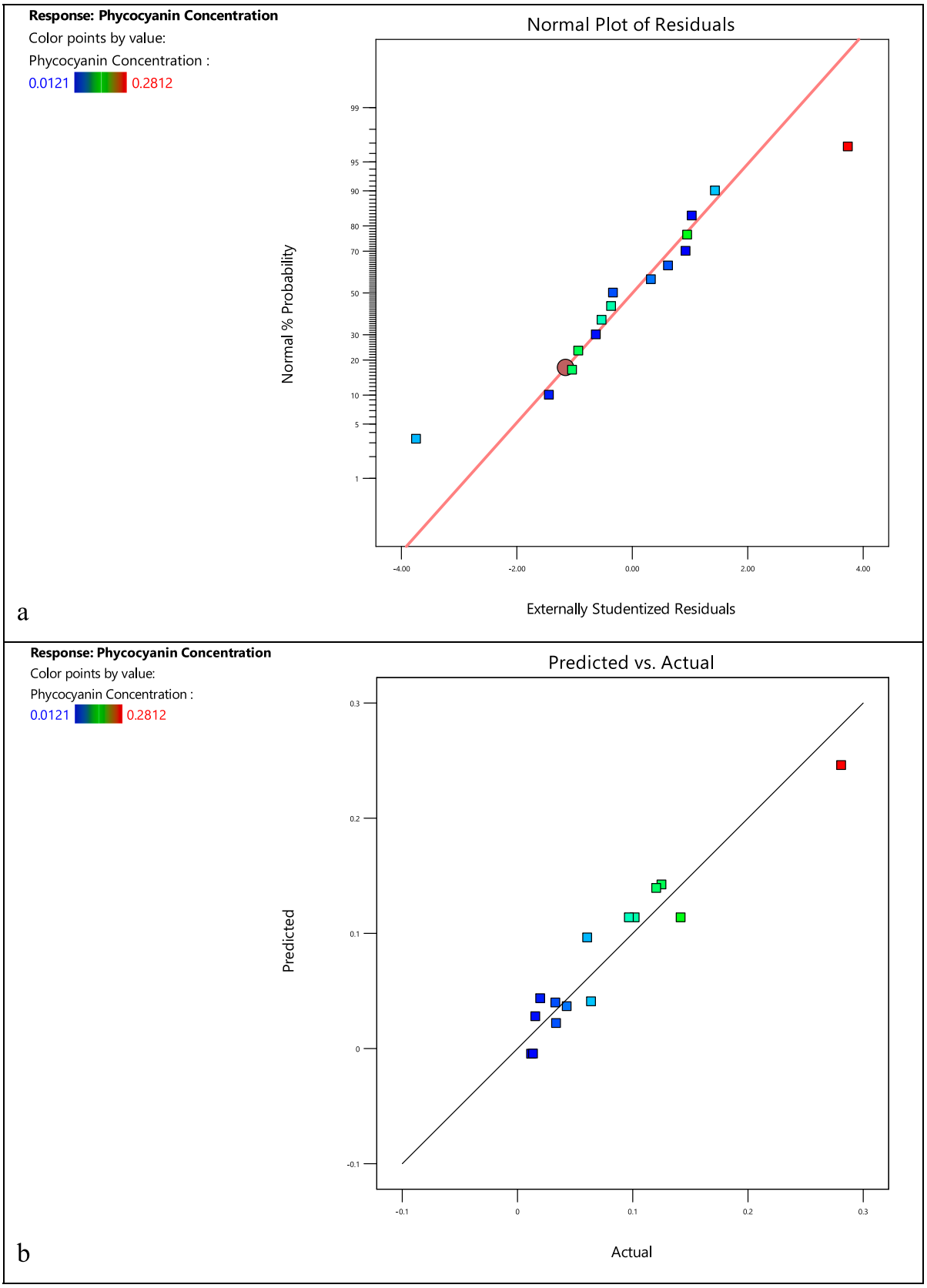

Fig. 2. Model diagnostic plots for Response 1. (a) Normal residual plot. (b) Predicted vs actual plot. [The predicted values align with the externally scrutinized values (a) and actual observed values (b), resulting in a scatter of data points along or near a 45-degree diagonal line (the line where predicted = actual). Deviations from the 45-degree line reveal the presence of bias in the model.].

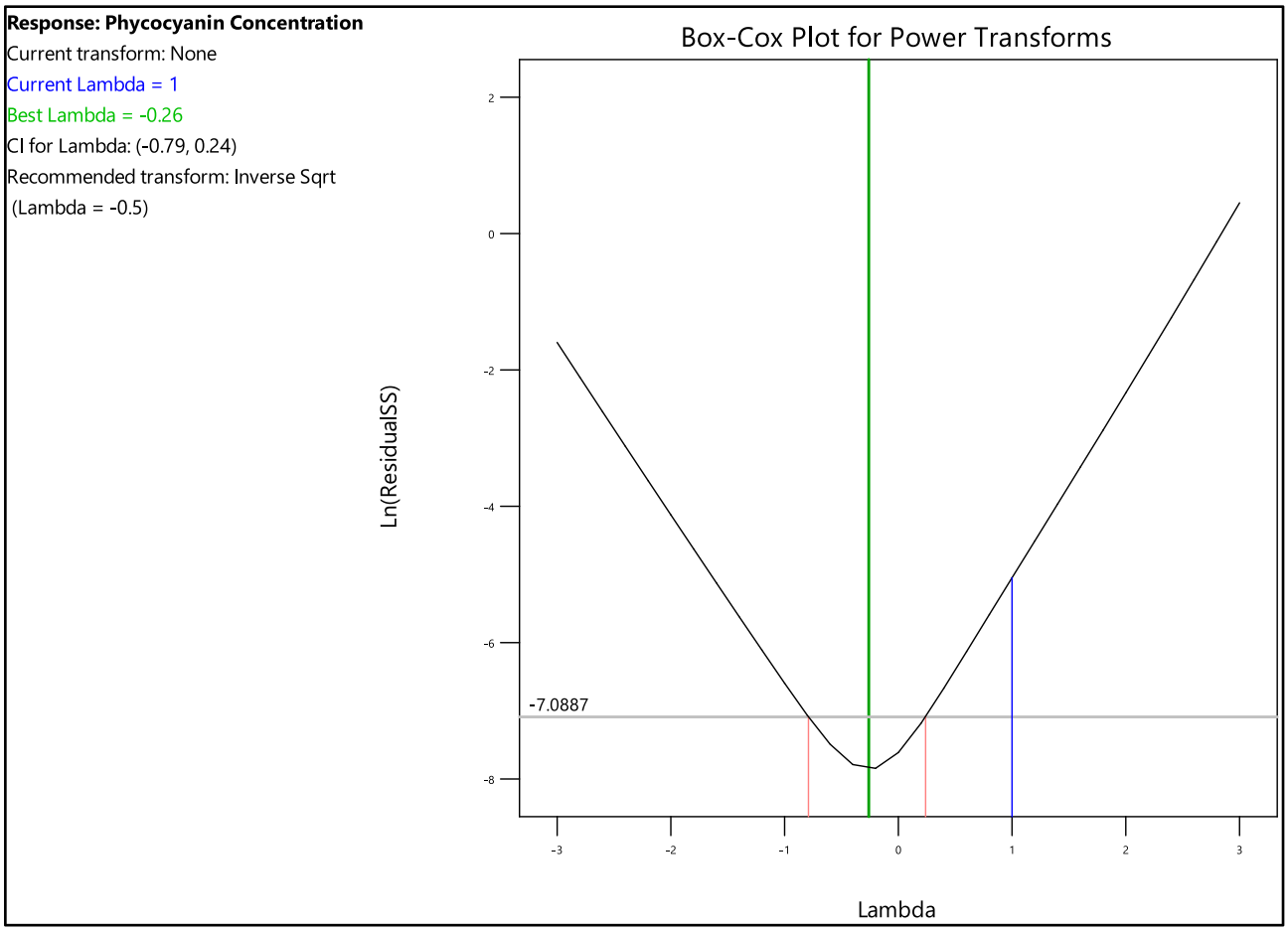

Fig. 3. Box-Cox Model Diagnostic Plot for Phycocyanin Concentration [The X-axis indicates λ = The optimal power transformation while the Y-axis represents the log of residuals.].

inhibit the activity of α-amylase and α-glucosidase enzymes. These findings will further facilitate in evaluating the antiglycating potential of Phycocyanin.

The extraction of phycocyanin can produce variable results attributed to inherent fluctuations in factors including the cell cycle, environmental conditions during organism growth, and methodological nuances (Li et al., 2020). These variations introduce unpredictability in extraction efficiency and impact the quality of phycocyanin (Betz et al., 2011). Quality by Design (QbD) is a systematic approach to product development and manufacturing, aiming to consistently produce high-quality products. It focuses on understanding and controlling critical parameters throughout the product lifecycle, promoting efficiency, risk management, and regulatory compliance (Yu et al., 2014). In the context of phycocyanin extraction, QbD is vital for optimizing processes and ensuring reliable and robust outcomes. The Box-Behnken Design, a response surface methodology, is particularly valuable in this pursuit. Its efficiency in exploring multiple variables simultaneously allows for the identification of optimal conditions, providing statistical rigor and versatility across various scientific fields (López et al., 2020), including the extraction of phycocyanin where it aids in systematically varying factors to enhance the overall efficiency and quality of the extraction process.

The authors observed a lack of research articles utilizing response surface methodology for optimizing phycocyanin extraction, where Silveira et al. (2007) employed factorial design. In contrast, our study takes a Quality by Design (QbD) approach, utilizing the Box-Behnken design to optimize the extraction of high-purity phycocyanin from Spirulina, highlighting a systematic approach to ensure product quality. We assess phycocyanin purity through Fourier-Transform Infrared Spectroscopy (FTIR) and confirm structural integrity using Sodium Dodecyl Sulfate-Polyacrylamide Gel Electrophoresis (SDS-PAGE). Additionally, we explore its antioxidant potential through various assays, which are crucial for applications in functional foods and pharmaceuticals. This study reveals that Spirulina-derived phycocyanin inhibits amylase and glucosidase enzymes, offering potential benefits in managing post-meal blood sugar levels for individuals with diabetes. Additionally, its antioxidant properties can help counteract oxidative stress, reducing the risk of diabetes-related complications. These findings suggest the potential use of phycocyanin as a natural intervention for post-meal blood sugar control and diabetes-related complications, opening avenues for further research and product development in this area.

2. Materials and Methods

2.1. Materials

Axenic culture of *Spirulina platensis* PCC 7345 was graciously provided as a gift by Dr. Vani B at BITS Pilani, Hyderabad. The growth medium BG11 was procured from Himedia Laboratories in Mumbai, India, while all other chemical reagents were purchased from SD Fine Chemicals, Mumbai, India.

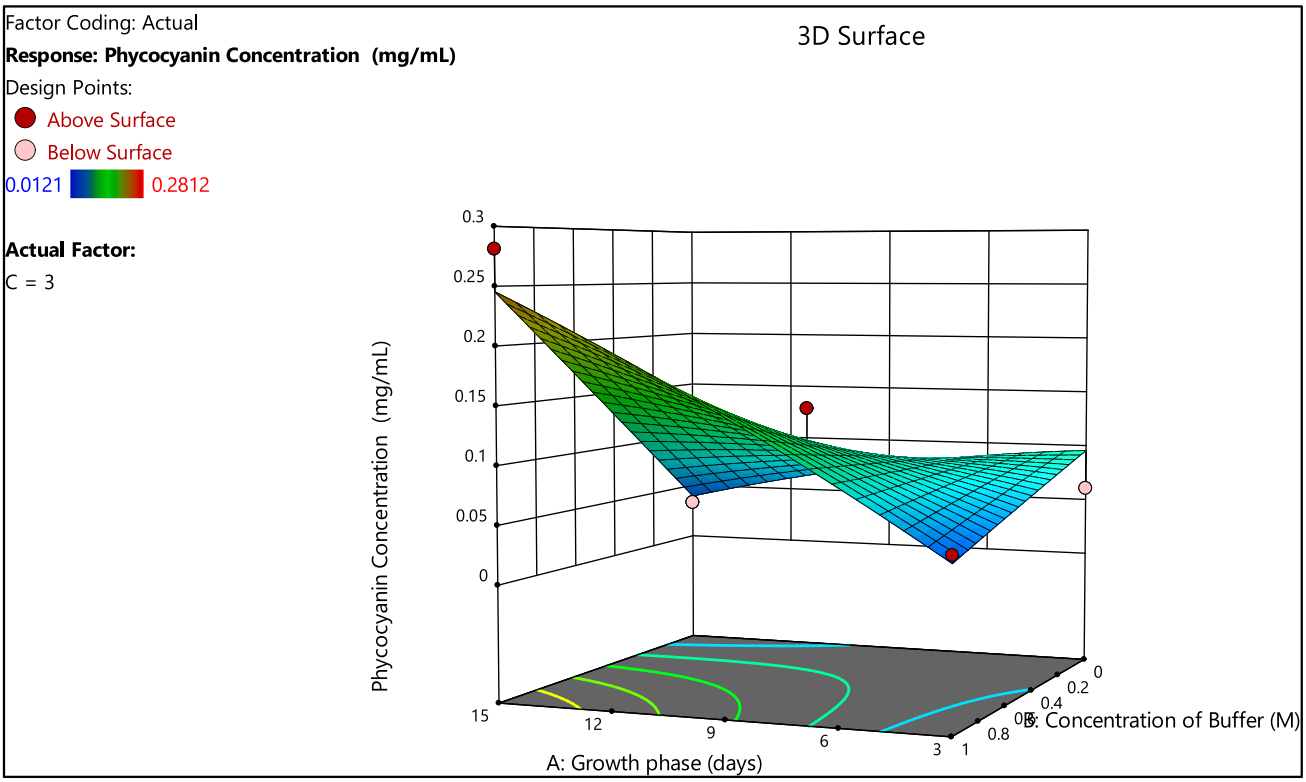

Fig. 4. Contour plots for factors affecting Phycocyanin concentration [Two factors namely A: Growth phase (days) and B: Concentration of Buffer (M) are represented in the X axes, Response: Phycocyanin concentration (mg/ml) is represented in Y axis.].

Table 3
Model Summary Statistics for Response 2.

Source	Std. Dev.	R^2	Adjusted R^2	Predicted R^2	PRESS	
Linear	0.1278	0.2403	0.0331	−0.6239	0.3841	
2FI	**0.1164**	**0.5416**	**0.1979**	**−1.4278**	**0.5742**	**Suggested**
Quadratic	0.1333	0.6242	−0.0523	−4.9811	1.41	
Cubic	0.0166	0.9977	0.9836		*	Aliased

2.2. QbD approach

2.2.1. Defining the TPPs and determination of CQAs

In the first stage of a Quality by Design (QbD) study, the primary focus is on identifying the potential target product profile (TPP) and the critical quality attributes (CQAs) of the formulation (Dhoble and Patravale, 2019). The selection of CQAs was informed by literature reports in the field of extraction and purification studies (Aoki et al., 2021; Asayama, 2012; Kuddus et al., 2013; Kumar et al., 2014; Seo et al., 2013; Wang et al., 2001). Accordingly, Phycocyanin concentration and purity were categorized as the final CQAs with a direct influence on the quality of Phycocyanin.

2.2.2. Risk evaluation

A risk evalution was conducted to determine factors that significantly impact the quality of phycocyanin during its extraction and optimization. To identify the critical material attributes (CMAs) and critical process parameters (CPPs), an Ishikawa fishbone diagram, often called a cause-and-effect diagram, was developed. Canva online software tool was used for drawing the diagram. Following the risk analysis and initial investigations, three vital factors affecting Phycocyanin quality were selected. Specifically, the molarity of the extraction buffer was identified as a CMA, while the number of freeze–thaw cycles and the growth phase of the *Spirulina platensis* culture were recognized as CPPs (Aoki et al., 2021; Asayama, 2012; Dhoble and Patravale, 2019; Kuddus et al., 2013; Kumar et al., 2014; Seo et al., 2013; Wang et al., 2001).

2.2.3. Experimental design

Response Surface methodology was employed to identify three variables for the optimization study using Design-Expert 13 software (Dhoble and Patravale, 2019). They were identified as the number of the growth phase of the cycle (days), freeze–thaw cycles, and molarity of buffer (M) and were designated as A, B, and C, respectively. These three factors were each tested at two levels and 3 center points. The influence of these variables on two response variables, namely, phycocyanin concentration (mg/ml) (Y1) and purity (Y2), and C-PC production, was studied using Box-Benken design.

2.2.4. Extraction of Phycocyanin

Phycocyanin was extracted after 14 days of growth from *Spirulina platensis* PCC 7345. The culture was incubated in St. BG11 medium with constant stirring at 100 rpm and continuous photoperiod. After incubation, the cell biomass was collected by centrifuging at 10000 rpm for 10 min at 10 °C. The organism's biomass was then washed with distilled water thrice. 5gm of biomass was weighed and transferred into a beaker containing 1 M sodium phosphate buffer (pH 7.0). This mixture was allowed to freeze for 12 h and then subjected to thawing at room temperature. After repeating the procedure twice, the mixture was centrifugated (Bennett and Bogorad, 1973; Tan et al., 2020)The supernatant was tested spectrophotometrically for Phycocyanin yield and purity

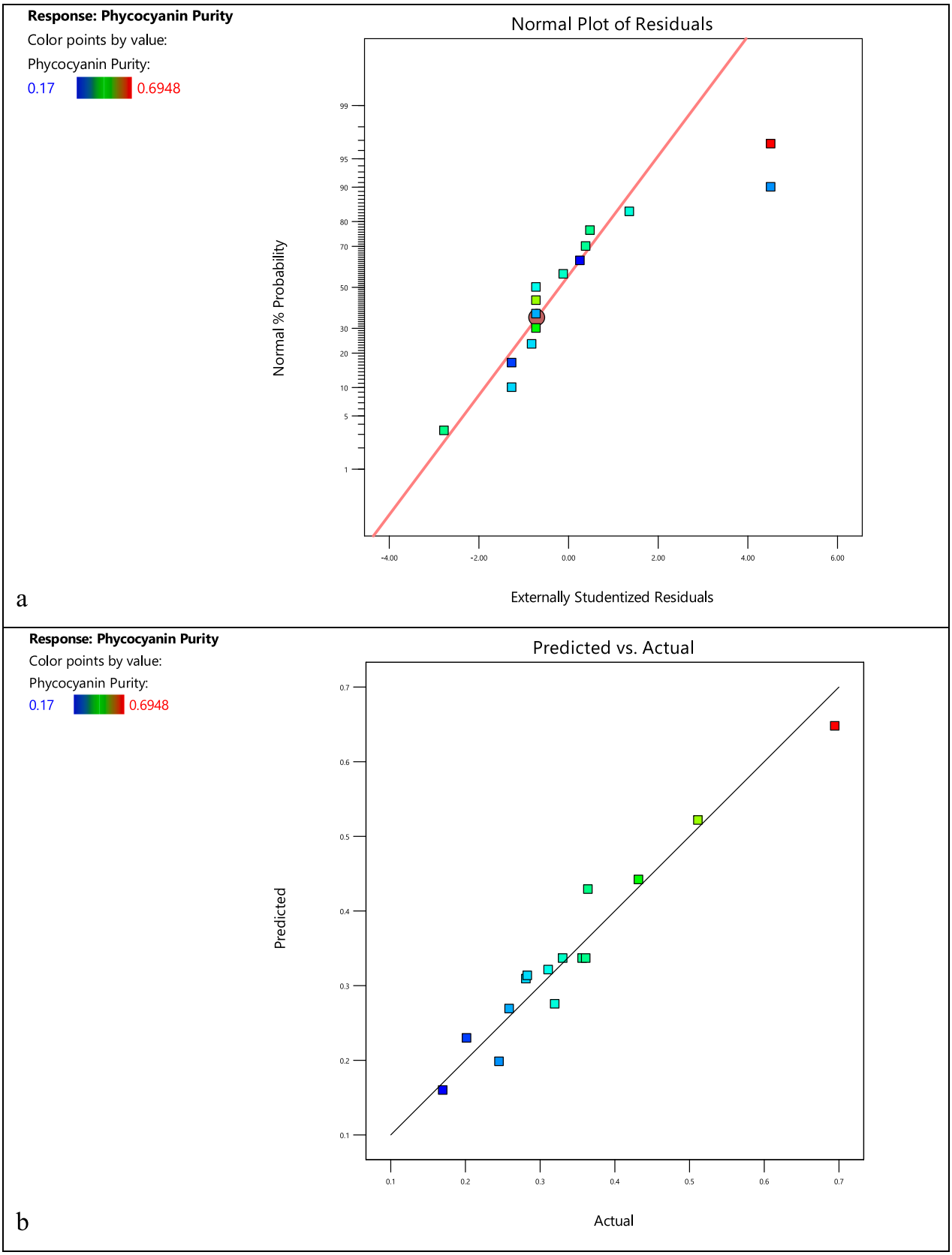

Fig. 5. Model diagnostic plots for Response 2. (a) Normal residual plot. (b) Predicted vs actual plot. [The predicted values align with the externally scrutinized values (a) and actual observed values (b), resulting in a scatter of data points along or near a 45-degree diagonal line (the line where predicted = actual).].

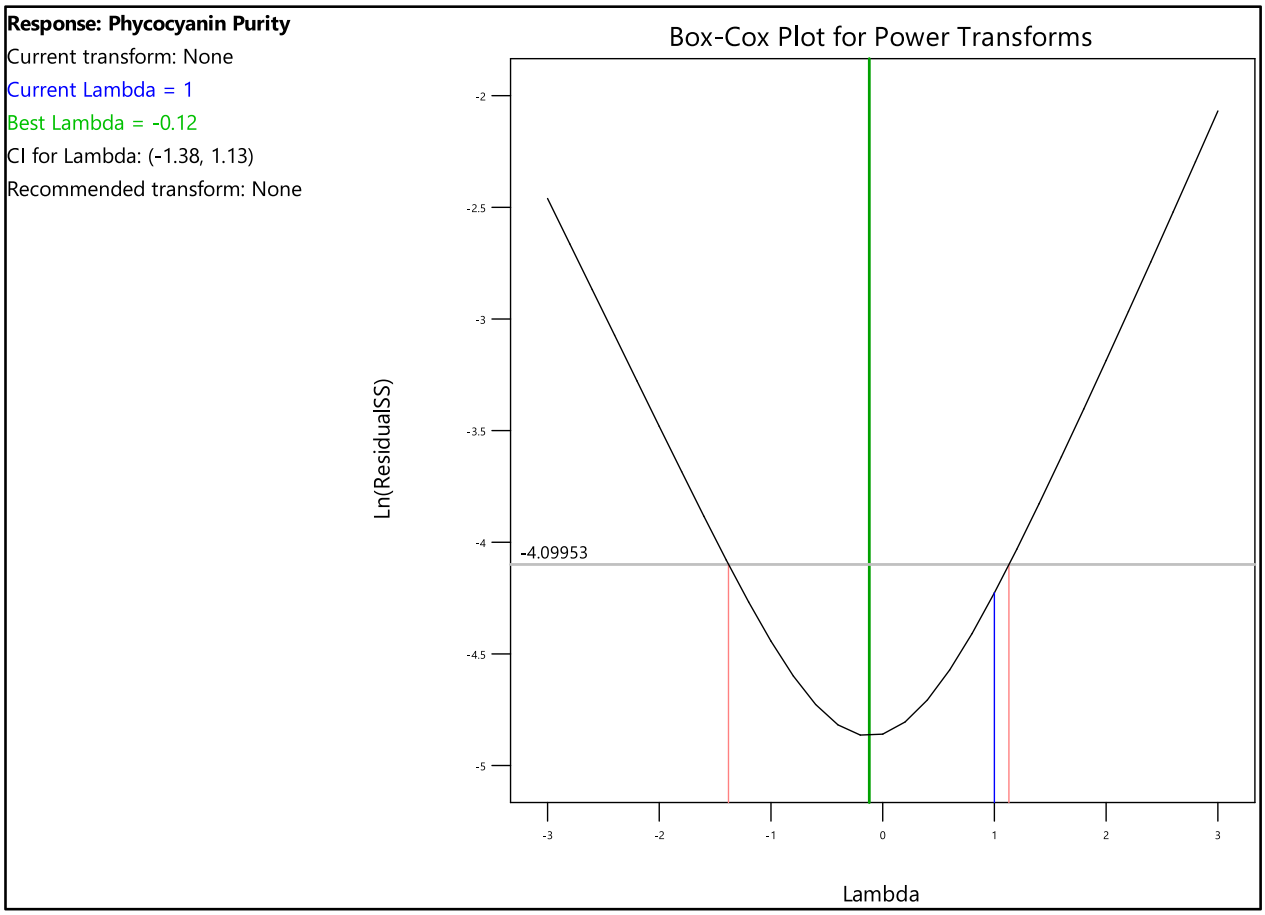

Fig. 6. Box-Cox Model Diagnostic Plot for Phycocyanin Purity [The X-axis indicates λ = The optimal power transformation while the Y-axis represents the log of residuals.].

using the following formulae:

Phycocyanin concentration (mg/ml) = [A620nm − 0.474 (A652nm)]/5.34 (Bennett and Bogorad, 1973).

Phycocyanin purity = A620nm/A280nm (Tan et al., 2020).

2.2.5. *Numerical optimisation of the design*

The experimental findings were scrutinized, and the procedure was fine-tuned to mitigate potential risks. This was accomplished through numerical optimization, which was subsequently complemented with the application of a point prediction technique (Dhoble and Patravale, 2019). Specific criteria were set for the experiment, involving the growth phase duration (3–15 days), extraction buffer concentration (0–1 M), and the number of freeze–thaw cycles (2–4). A software tool suggested 15 runs, and one was chosen for point prediction and validated through triplicate testing. Target values for Phycocyanin yield (0.1–0.3 mg/ml) and purity (0.1–1.0) were established. The selected run had a growth phase of 11.31 days, extraction buffer concentration at 0.7920 M, and 2.17 freeze–thaw cycles, resulting in a predicted Phycocyanin concentration of 0.08 mg/ml and a purity of 0.407. This was confirmed through triplicate runs, and the results were compared with the predictions.

2.3. *FTIR analysis of the extracted Phycocyanin*

The extracted Phycocyanin's Fourier transform infrared (FTIR) spectrum was carried out using a 3000 Hyperion Microscope with Vertex 80 FTIR System (Bruker, Germany). The obtained peaks were analyzed by referencing a standard IR spectra table (Balyan et al., 2022).

2.4. *SDS PAGE for confirmation of the presence of Phycocyanin subunits*

The Phycocyanin sample (20 µL) was combined with 20 µL SDS-sample buffer. The mixture was then subjected to heating at 60 °C for a duration of 3 min. Subsequently, an aliquot of 10 µL from the final mix was utilized for electrophoresis. The prepared samples were loaded onto gels containing a tracking dye, with a stacking gel of 5% and a resolving gel of 15%. Electrophoresis was conducted at a constant voltage of 80 V to separate the proteins based on their molecular weight. After electrophoresis, the gels were stained for 60 min using a bromophenol blue dye solution to visualize the separated proteins. Subsequently, the gels were de-stained using standard procedures to remove excess dye, ensuring the protein bands were visible. Finally, the gels were imaged for further analysis (Kumar and Ali, 2019).

2.5. *GC analysis of the extracted Phycocyanin*

Gas chromatography (GC) was employed for the comprehensive qualitative and quantitative analysis of organic compounds present in the extract. The potential bioactive constituents were scrutinized using a GC system. The gas chromatography (GC) component employed an Agilent 7890-Jeol: AccuTOF GCV instrument with an Elite 1 column, a Flame Ionization Detector (FID), a headspace injector, and a Combipal autosampler. Helium gas served as the carrier gas, flowing at a rate of 1 ml/min. The injector volume was set at 2 µL, and the injector temperature was maintained at 280 °C. The oven temperature was programmed to increase from 40 to 280 °C with an isothermal period of 5 min. Identification of bioactive compounds was accomplished by assessing retention time and the percentage contribution of these compounds

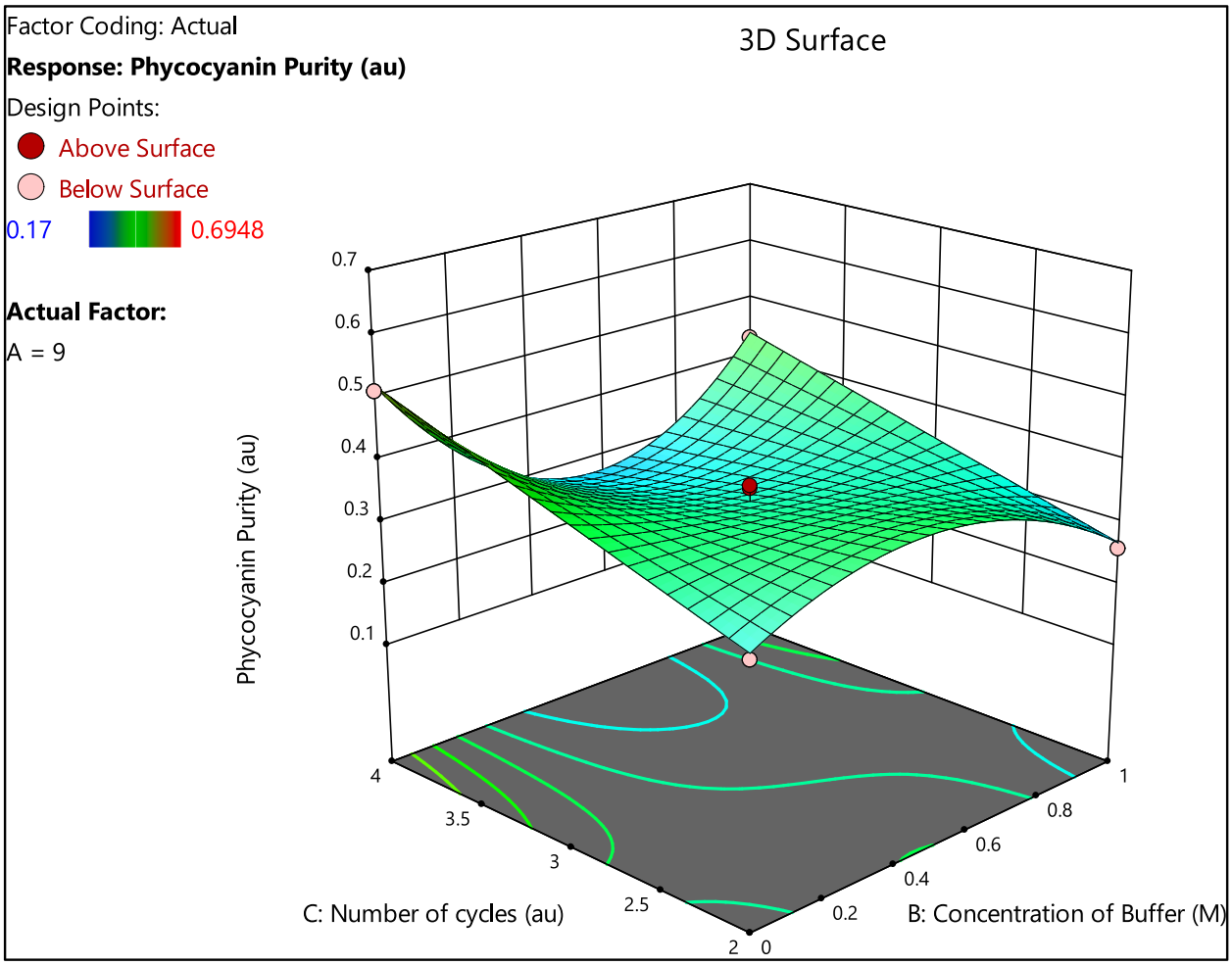

Fig. 7. Contour plots for factors affecting Phycocyanin Purity [Two factors namely B: Concentration of Buffer (M) and C: Number of freeze–thaw cycles (arbitrary units) are represented in the X axes, Response: Phycocyanin Purity (au) is represented in Y axis.].

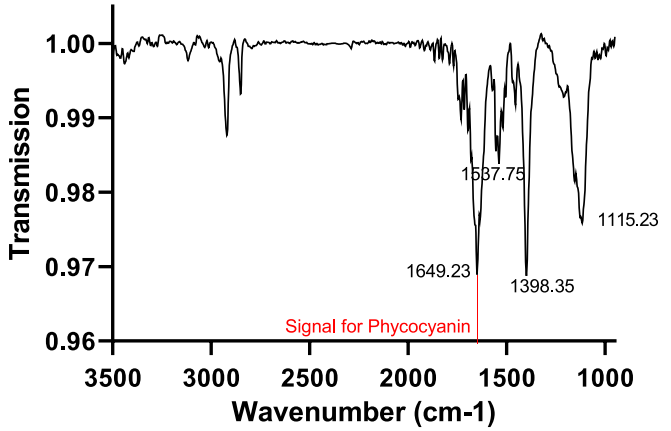

Fig. 8. FTIR spectrum for phycocyanin extract shows a transmittance maxima at 1649 cm^{-1} [Graph of Transmittance (%) vs wavenumber (cm^{-1}) shows maximum transmittance at 1649 cm^{-1}. This corresponds to the signal emitted by phycocyanin at 1651 cm^{-1}.].

based on the total peak area (Chirumamilla et al. 2022).

2.6. Determining antioxidant potential of Phycocyanin

The capacity of phycocyanin to scavenge free radicals was assessed

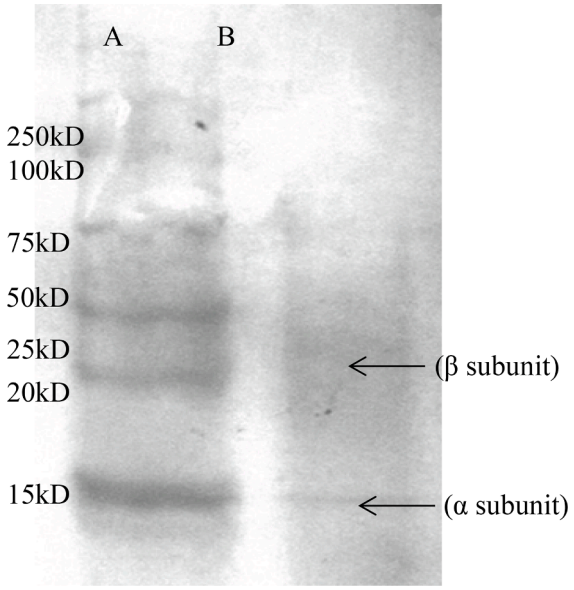

Fig. 9. SDS-PAGE displaying subunits of Phycocyanin [Lane A: Protein Ladder, Lane B: Extracted and Purified Phycocyanin].

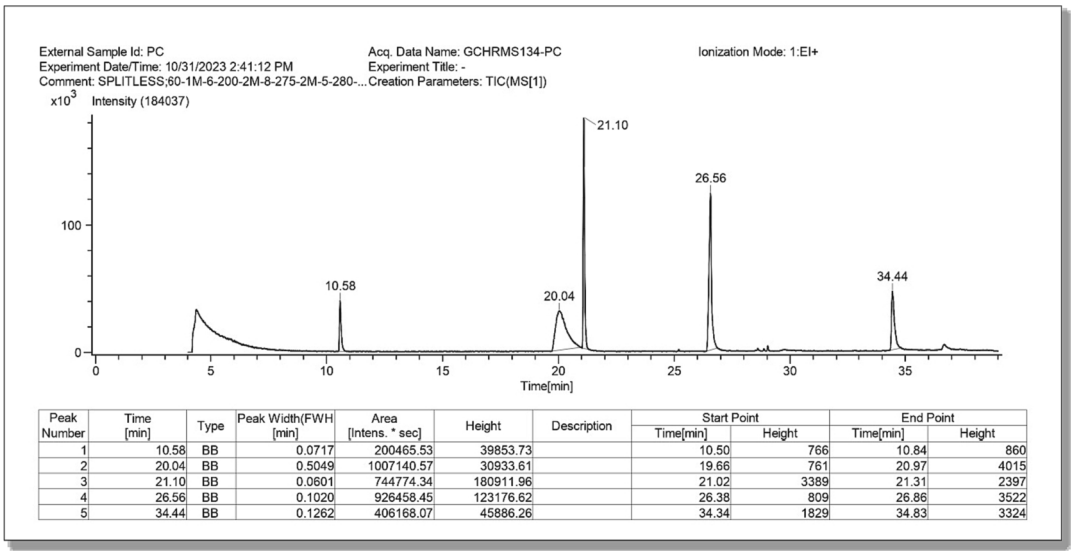

Peak Number	Time [min]	Type	Peak Width(FWH [min]	Area [Intens. * sec]	Height	Description	Start Point		End Point	
							Time[min]	Height	Time[min]	Height
1	10.58	BB	0.0717	200465.53	39853.73		10.50	766	10.84	860
2	20.04	BB	0.5049	1007140.57	30933.61		19.66	761	20.97	4015
3	21.10	BB	0.0601	744774.34	180911.96		21.02	3389	21.31	2397
4	26.56	BB	0.1020	926458.45	123176.62		26.38	809	26.86	3522
5	34.44	BB	0.1262	406168.07	45886.26		34.34	1829	34.83	3324

Fig. 10. GC Spectrum of Phycocyanin [Graph of Intensity VS time in mins].

by implementing the 2, 2-Diphenyl-1-picrylhydrazyl (DPPH) assay. Additionally, the ability to counter nitric oxide radicals was evaluated using a freshly prepared Greiss reagent. In this evaluation, varying concentrations of phycocyanin (ranging from 20 µg/ml to 100 µg/ml) were combined with a pre-prepared solution of 2, 2′-casino-bis (3-ethylbenzothiazoline-6-sulfonic acid) (ABTS. +) and subjected to a 30-minute incubation period at 734 nm (Balyan et al., 2022; Paramanya et al., 2023a). These observations were further compared to a reference antioxidant, ascorbic acid.The subsequent determination of percentage inhibition for all three assays was accomplished by applying the following calculation:

$$\%\ \text{Inhibition} = \frac{\text{Abs Control} - \text{Abs phycocyanin}}{\text{Abs Control}} \times 100$$

2.7. Evaluation of enzyme inhibition property

2.7.1. α-Amylase inhibition assay

The modified approach, as outlined by Sathiavelu and colleagues (2013), aimed to assess the inhibitory effects of phycocyanin in a concentration range of 0 to 100 µg/ml on α-amylase activity. Acarbose, used as a standard, was also tested in the same concentration range (0 to 100 µg/ml).

$$\%\ \text{Inhibition of}\ \alpha - \text{amylase} = \frac{\text{AC} - \text{AP}}{\text{AC}} \times 100$$

In this equation, AC represents the absorbance of the control, which lacked phycocyanin, while AP represents the absorbance of the test sample containing phycocyanin. This calculation determined the extent to which phycocyanin inhibited α-amylase activity, providing valuable insights into its potential as an inhibitory agent.

2.7.2. α-Glucosidase inhibition assay

The impact of phycocyanin at a concentration of 100 µg/ml on α-glucosidase activity was assessed using the method outlined in a previous study (Kazeem et al., 2013). Acarbose was employed as a standard and tested over a concentration range of 0 to 1000 µg/ml.

$$\%\ \text{Inhibition of}\ \alpha - \text{Glucosidase} = \frac{\text{AC} - \text{AP}}{\text{AC}} \times 100$$

Here, AC denotes the absorbance of the control sample, which did not contain phycocyanin, while AP represents the absorbance of the test sample containing phycocyanin.

2.8. Statistical analysis

The analysis was performed using Graph Pad Prism version 9 software. The statistical significance of the data was assessed through a two-way analysis of variance (ANOVA). The data were presented as the mean ± standard deviation (SD) with a sample size of n = 3. Tukey's multiple comparisons tests were employed to assess variances between different treatments. Statistical significance was indicated by a value of $p < 0.05$ when compared against the positive control group [Balyan and Ali, 2022; Paramanya et al., 2023a].

3. Results

3.1. Quality by Design approach

3.1.1. Defining the TPPs and determination of CQAs

In our study, we adopted a QbD approach for extracting Phycocyanin from *Spirulina platensis* PCC 7345. This approach necessitated carefully considering various TPPs based on an extensive literature review. As a critical step in the QbD framework, we established a set of CQAs that directly impact the purity and quality of the extracted Phycocyanin. After comprehensive evaluation, it was determined that Phycocyanin concentration and purity would serve as the ultimate CQAs, as they play a pivotal role in ensuring the quality of the Phycocyanin product. These CQAs were chosen based on their direct influence on the final product's integrity and suitability for various applications (Kumar et al. 2014, Seo et al., 2013).

3.1.2. Risk evaluation

The CQAs chosen for assessment were Phycocyanin concentration and purity. Consequently, it was imperative to assess the potential factors that could influence these primary product qualities. To identify these factors, Ishikawa diagrams (also known as cause and effect diagrams) were created, as illustrated in Fig. 1. The Ishikawa diagram revealed that the concentration of the buffer, the duration of the culture's growth phase, and the number of freeze–thaw cycles were identified as factors with a significant impact on Phycocyanin concentration and purity, as indicated in references (Asayama et al., 2012; Kuddus et al., 2013).

3.1.3. Box Behnken design

The Box-Behnken design was utilized, and Design Expert software was employed to analyze the impact of different factors on the response

Table 4
Result of GCMS.

Retention Time	Hit	Compound name	Molecular Formula	Match Factor (MF)	Reverse Match Factor (RMF)	ID in mainlib database
10.58	1	5H-Cyclopropa(3,4)benz(1,2-e)azulen-5-one, 1,1a-α,1b-β,4,4a,7a-α,7b,8,9,9a-decahydro-7b-α,9-β,9a-α-trihydroxy	C41H66O8	495	663	21221
	2	Decanoic acid, 1,1a,1b,4,4a,5,7a,7b,8,9-decahydro-4a,7b-dihydroxy-1,1,6,8-tetramethyl-5-oxo-3-[[(1-oxodecyl)oxy]methyl]-9	C41H66O8	458	542	5809
	3	1′,1′-Dicarboethoxy-1β,2β-dihydro-3′H-cycloprop[1,2]cholesta-1,4,6-trien-3-one	C34H50O5	456	698	5215
	4	2β,4a-Epoxymethylphenanthrene-7-methanol, 1,1-dimethyl-2-methoxy-8-(1,3-dithiin-2-ylidene)methyl-1,2,3,4,4a,4b,5,6,7,8,8	C27H38O4S2	453	765	190470
	5	Carda-16,20(22)-dienolide, 3-[(6-deoxy-3,4-O-methylenehexopyranos-2-ulos-1-yl)oxy]-7,8-epoxy-11,14-dihydroxy-12-oxo-, (3.beta.,5.beta.,7.beta.,11.alpha.)-	C30H36O11	451	794	19022
	6	9-Octadecenoic acid (Z)-, 3-[(1-oxohexadecyl)oxy]-2-[(1-oxooctadecyl)oxy]propyl ester	C55H104O6	429	564	191098
	7	3′H-Cycloprop(1,2)-5α-cholest-1-en-3-one, 1′,1′-dicarboethoxy-1β,2β-dihydro-	C34H54O5	426	629	186161
	8	Octadecanoic acid, 1-[[(1-oxohexadecyl)oxy]methyl]-1,2-ethanediyl ester	C55H106O6	425	554	22164
20.04	1	Decanoic acid, 1,1a,1b,4,4a,5,7a,7b,8,9-decahydro-4a,7b-dihydroxy-3-(hydroxymethyl)-1,1,6,8-tetramethyl-5-oxo-9aH-cyclopropa[3,4]benz[1,2-e]azulene-9,9a-diyl ester, [1aR-(1aalpha,1bbeta,4abeta,7aalpha,7balpha,8alpha,9beta,9aalpha)]-	C50H82O9	375	436	5809
	2	4a-Phorbol 12,13-didecanoate	C40H64O8	328	496	27185
	3	Hexadecanoic acid, 1a,2,5,5a,6,9,10,10a-octahydro-5,5a-dihydroxy-4-(hydroxymethyl)-1,1,7,9-tetramethyl-11-oxo-1H-2,8a-methanocyclopenta[a]cyclopropa[e]cyclodecen-6-yl ester, [1aR-(1aalpha,2alpha,5beta,5abeta,6beta,8aalpha,9alpha,10aalpha)]-	C36H58O6	302	434	169962
	4	Cholestan-3-ol, 5-chloro-6-nitro-, acetate (ester), (3β,5α,6β)-	C29H48ClNO4	301	561	13491
	5	3-Pyridinecarboxylic acid, 2,7,10-tris(acetyloxy)-1,1a,2,3,4,6,7,10,11,11a-decahydro-1,1,3,6,9-pentamethyl −4-oxo-4a,7a-epoxy-5H-cyclopenta[a]cyclopropa[f]cycloundecen-11-yl ester, [1aR-(1aR*,2R*,3S*,4aR*,6S*,7S*,7aS*,8E,10R*,11R*,11aS*)]-	C32H39NO10	295	447	6247
	6	Decanoic acid, 1,1a,1b,4,4a,5,7a,7b,8,9-decahydro-4a,7b-dihydroxy-3-(hydroxymethyl)-1,1,6,8-tetramethyl −5-oxo-9aH-cyclopropa[3,4]benz[1,2-e]azulene-9,9a-diyl ester, [1aR-(1aα,1bβ,4aβ,7aα,7bα,8α,9β,9aα)]-	C40H64O8	294	510	6718
	6	Spiro[cyclohexane-1,6′-[2]oxabicyclo[3.2.0]heptan]-3′-one, 4′-cyclohexylidene-7′-(Z)-(4-hexadecanoyloxybenzoylmethylene)-1′-(4-hexadecanoyloxyphenyl)	C63H92O7	289	440	84646
	7	Pentacyclo[19.3.1.1(3,7)0.1(9,13)0.1(15,19)]octacosa-1(25),3,5,7(28),9,11,13(27),15,17,19(26),21,23-dodecaene-25,26,27,28-tetrol, 5,11,17,23-tetrakis(1,1-dimethylethyl)	C44H56O4	284	516	5967
	8	Docosanoic acid, 1,2,3-propanetriyl ester	C69H134O6	274	558	2816
	9	8-Acetoxy-5b-methylperhydrocyclobuta[n]phenanthrene-11-ol-2,3-dione-2a-propanoic acid lactone	C22H28O6	264	624	13412
21.10	1	5H-Cyclopropa(3,4)benz(1,2-e)azulen-5-one, 1,1a-α,1b-β,4,4a,7a-α,7b,8,9,9a-decahydro-7b-α,9-β,9a-α-trihydroxy-3-hydroxymethyl-1,1,6,8-α-tetramethyl-4a-methoxy-, 9,9a-didecanoate	C41H66O8	624	726	21221
	2	4a-Phorbol 12,13-didecanoate	C40H64O8	551	664	27185
	3	Octadecanoic acid, 1-[[(1-oxohexadecyl)oxy]methyl]-1,2-ethanediyl ester	C55H106O6	544	628	22164
	4	Octadecane, 3-ethyl-5-(2-ethylbutyl)-	C26H54	541	753	7340
	5	Octadecanoic acid, 3-[(1-oxohexadecyl)oxy]-2-[(1-oxotetradecyl)oxy]propyl ester	C51H98O6	538	691	21877
	6	Tetracosane, 12-decyl-12-nonyl-	C43H88	521	746	21916
	7	Tetratetracontane	C44H90	524	757	5519
	8	Decanoic acid, 1,1a,1b,4,4a,5,7a,7b,8,9-decahydro-4a,7b-dihydroxy-3-(hydroxymethyl)-1,1,6,8-tetramethyl-5-oxo-9aH-cyclopropa[3,4]benz[1,2-e]azulene-9,9a-diyl ester, [1aR-(1aα,1bβ,4aβ,7aα,7bα,8α,9β,9aα)]-	C40H64O8	524	663	6718
	9	Heptadecane, 9-hexyl-	C23H48	517	778	7302
	10	Octadecanoic acid, 2-[(1-oxotetradecyl)oxy]-1,3-propanediyl ester	C53H102O6	515	679	21858
26.56	1	Decanoic acid, 1,1a,1b,4,4a,5,7a,7b,8,9-decahydro-4a,7b-dihydroxy-1,1,6,8-tetramethyl-5-oxo-3-[[(1-oxodecyl)oxy]methyl]-9aH-cyclopropa[3,4]benz[1,2-e]azulene-9,9a-diyl ester, [1aR-(1aα,1bβ,4aβ,7aα,7bα,8α,9β,9aα)]-	C50H82O9	528	627	5809
	2	4a-Phorbol 12,13-didecanoate	C40H64O8	505	730	27185
	3	Docosanoic acid, 1,2,3-propanetriyl ester	C69H134O6	459	812	2816
	4	Decanoic acid, 1,1a,1b,4,4a,5,7a,7b,8,9-decahydro-4a,7b-dihydroxy-3-(hydroxymethyl)-1,1,6,8-tetramethyl-5-oxo-9aH-cyclopropa[3,4]benz[1,2-e]azulene-9,9a-diyl ester, [1aR-(1aα,1bβ,4aβ,7aα,7bα,8α,9β,9aα)]-	C40H64O8	458	757	6718
	5	Hexadecanoic acid, 1a,2,5,5a,6,9,10,10a-octahydro-5,5a-dihydroxy-4-(hydroxymethyl)-1,1,7,9-tetramethyl-11-oxo-1H-2,8a-methanocyclopenta[a]cyclopropa[e]cyclodecen-6-yl ester, [1aR-(1aα,2α,5β,5aβ,6β,8aα,9α,10aα)]-	C36H58O6	430	604	169962
	6	Acetic acid, 17-(4-hydroxy-5-methoxy-1,5-dimethylhexyl)-4,4,10,13,14-pentamethyl-2,3,4,5,6,7,10,11,12,13,14,15,16,17-tetradecahydrocyclopenta[a]phenanthryl ester	C33H56O4	429	713	34865
	7	Octadecanoic acid, 2-[(1-oxohexadecyl)oxy]-1-[[(1-oxohexadecyl)oxy]methyl]ethyl ester	C53H102O6	422	608	21985
	8	Octadecanoic acid, 2-[(1-oxotetradecyl)oxy]-1,3-propanediyl ester	C53H102O6	414	645	21858
	9	1,3-Dipalmitin trimethylsilyl ether	C38H76O5Si	403	672	28050
	10	Octadecanoic acid, 2-[(1-oxododecyl)oxy]-1,3-propanediyl ester	C51H98O6	397	613	21974
34.44	1	9-Octadecenoic acid (Z)-, 3-[(1-oxohexadecyl)oxy]-2-[(1-oxooctadecyl)oxy]propyl ester	C55H104O6	462	644	191098

(*continued on next page*)

Table 4 (*continued*)

Retention Time	Hit	Compound name	Molecular Formula	Match Factor (MF)	Reverse Match Factor (RMF)	ID in mainlib database
	2	Octadecanoic acid, 1-[[(1-oxohexadecyl)oxy]methyl]-1,2-ethanediyl ester	C55H106O6	453	623	22164
	3	5H-Cyclopropa(3,4)benz(1,2-e)azulen-5-one, 1,1a-α,1b-β,4,4a,7a-α,7b,8,9,9a-decahydro-7b-α,9-β,9a-α-trihydroxy-3-hydroxymethyl-1,1,6,8-α-tetramethyl-4a-methoxy-, 9,9a-didecanoate	C41H66O8	448	647	21221
	4	Decanoic acid, 1,1a,1b,4,4a,5,7a,7b,8,9-decahydro-4a,7b-dihydroxy-1,1,6,8-tetramethyl-5-oxo-3-[[(1-oxodecyl)oxy]methyl]-9aH-cyclopropa[3,4]benz[1,2-e]azulene-9,9a-diyl ester, [1aR-(1aα,1bβ,4aβ,7aα,7bα,8α,9β,9aα)]-	C50H82O9	444	556	5809
	5	2β,4a-Epoxymethylphenanthrene-7-methanol, 1,1-dimethyl-2-methoxy-8-(1,3-dithiin-2-yli-dene)methyl-1,2,3,4,4a,4b,5,6,7,8,8a,9-dodecahydro-, acetate	C27H38O4S2	431	792	190470
	6	1′,1′-Dicarboethoxy-1β,2β-dihydro-3′H-cycloprop[1,2]cholesta-1,4,6-trien-3-one	C34H50O5	424	707	5215
	7	3-Phorbinepropanoic acid, 9-acetyl-14-ethyl-13,14-dihydro-21-(methoxycarbonyl)-4,8,13,18-tetramethyl-20-oxo-, 3,7,11,15-tetramethyl-2-hexadecenyl ester	C55H76N4O6	414	566	24447
	8	3′H-Cycloprop(1,2)-5α-cholest-1-en-3-one, 1′,1′-dicarboethoxy-1β,2β-dihydro-	C34H54O5	410	661	186161
	9	Octadecanoic acid, 2-[(1-oxohexadecyl)oxy]-1-[[(1-oxohexadecyl)oxy]methyl]ethyl ester	C53H102O6	389	617	5581
	10	Docosanoic acid, 1,2,3-propanetriyl ester	C69H134O6	388	801	2816

[MF = comparison of the unknown's mass spectrum's peaks to those of the peaks in the library's spectra. RMF = match factor when the peaks in the unknown's spectrum that are not in the library's known reference spectrum are ignored. Interpretation: >900 = Excellent, 800–900 = Good, 700–800 = Fair, and < 600 = Poor match.].

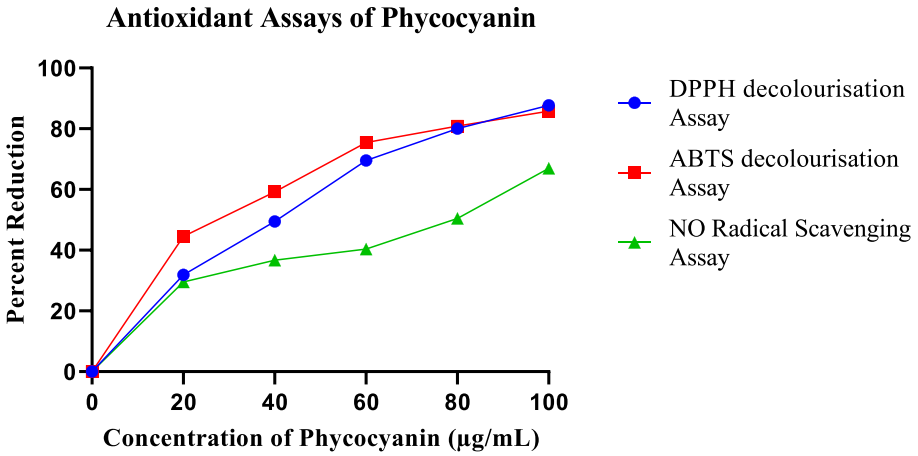

Fig. 11. Antioxidant Potential of Phycocyanin [Results expressed in the percentage of inhibition; mean (n = 3), $p < 0.05$.].

Table 5
Determining IC50 value for antioxidant assays.

	DPPH		ABTS		NO	
	Phycocyanin	Standard	Phycocyanin	Standard	Phycocyanin	Standard
Equation from Graph	y = 0.7118x + 21.028	y = 0.3942x + 19.811	y = 0.5217x + 37.87	y = 0.6088x + 10.998	y = 0.443x + 18.216	y = 0.4622x + 32.138
R^2	0.9667	0.9858	0.9368	0.9596	0.9239	0.9743
IC_{50} (µg/ml)	40.7024	76.58	23.25091	64.063	71.7471	38.65

[Standard: Ascorbic acid].

variables: Phycocyanin concentration and purity. The experimental matrix consisted of 15 distinct criterias, as detailed in Table 1. Within this matrix, Phycocyanin concentration ranged from 0.0121 to 0.2812 mg/ml, while purity ranged from 0.17 to 0.6948. The remaining data points were evenly distributed across this specified range, as referenced in sources (Aoki et al., 2021; Asayama, 2012; Dhoble and Patravale, 2019; Kuddus et al., 2013; Kumar et al., 2014; Seo et al., 2013; Wang et al., 2001).

3.1.3.1. Response 1. In the case of Phycocyanin concentration, the software examined four mathematical models, which included the linear model, 2FI model, cubic model, and quadratic model. Among these options, the quadratic model was recommended for its higher predictive power, whereas the cubic model was identified alliased (as indicated in Table 2). Following the application of ANOVA, the quadratic model was confirmed to be statistically significant, and the lack of fit ($p < 0.05$) was deemed non-significant.

A model diagnostic plot is a standard tool in statistics and data analysis, particularly for evaluating the effectiveness of predictive models like linear regression models. It helps assess how well the model's predictions align with the actual data (Dhoble and Patravale, 2019). In Fig. 2, the data points are distributed close to or along the diagonal line, indicating a good fit of the model. Since there are no noticeable deviations from the 45-degree line, we can infer that the model does not exhibit any bias.

The Box-Cox transformation is a family of power transformations used to stabilize variance and make data conform more closely to a normal distribution (Dhoble and Patravale, 2019). The λ for the given

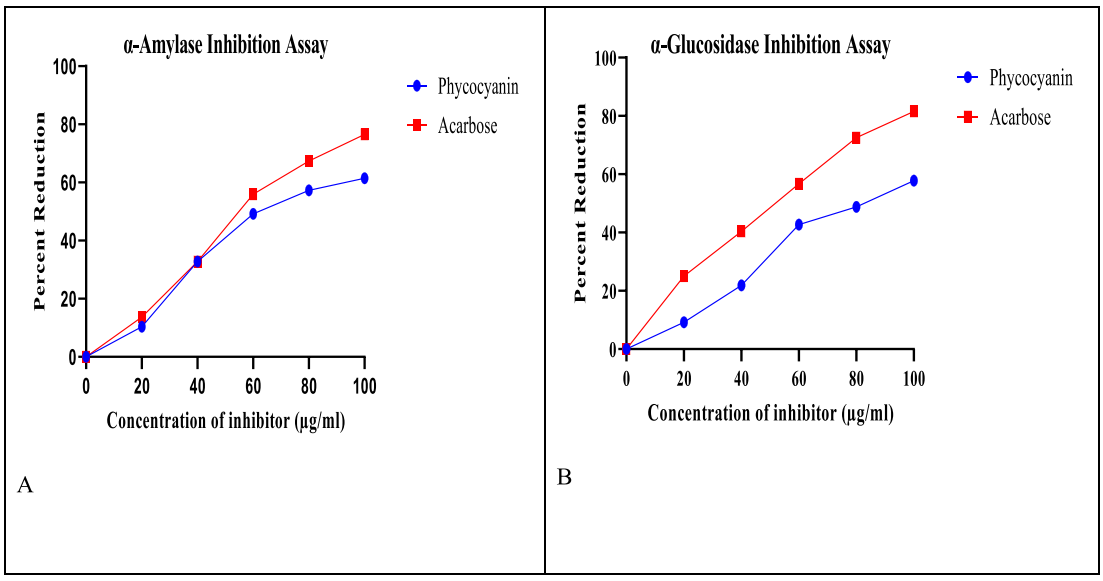

Fig. 12. Enzyme Inhibitory assays (A) α-amylase percent inhibition and (B) α-glucosidase percent inhibition [Results expressed in the percentage of inhibition; mean (n = 3), $p < 0.05$.].

Table 6
Determining IC50 value for enzyme inhibition assays.

	α-Amylase	α-Glucosidase
Equation from Graph	y = 0.6332x + 4.2546	y = 0.6202x − 1.1349
R^2	0.917	0.9616
IC_{50} (µg/ml)	72.24	82.45

data set = 1, the software suggests the fit for the data should be at λ = −0.26. The suggested transformation for the current data set is inverse square root which will improve the model fitness.

The final equation describing the response1 is Phycocyanin concentration (mg/ml) = −0.395093–0.011435* Growth phase −0.199347* Concentration of Buffer + 0.340080* Number of cycles + 0.022150 (Growth phase * Concentration of Buffer) + 0.003658 (Growth phase * Number of cycles) + 0.025200 (Concentration of Buffer * Number of cycles) −0.000236 Growth phase^2 −0.002353 Concentration of Buffer^2 −0.058388 Number of cycles^2 (Fig. 2, Fig. 3, Fig. 4).

3.1.3.2. Response 2. Regarding Phycocyanin purity, the software evaluated four mathematical models, specifically the linear model, 2FI model, cubic model, and quadratic model. Among these models, the 2FI model was identified as having the highest predictive power, while the cubic model was observed to be aliased, as indicated in Table 3. Subsequent ANOVA analysis confirmed the significance of the 2FI model, and it was determined that the lack of fit ($p < 0.05$) was not significant.

Fig. 5 displays data points that are closely aligned with or clustered around the diagonal line, suggesting a strong model fit. The absence of significant deviations from the 45-degree line leads us to conclude that the model is devoid of any noticeable bias.

The Box-Cox Model Diagnotic Plot for Phycocyanin Purity, the λ for the given data set = 1, the software suggests the fit for the data should be at λ = -0.12. The software considers the model as fit and does not recommend any teansformations.

The final equation describing the response 2 is Phycocyanin purity = -0.173547 + 0.074605* Growth phase + 1.74942*Concentration of Buffer + 0.100200* Number of cycles-0.081383 *(Growth phase * Concentration of Buffer)-0.618200* (Concentration of Buffer * Number of cycles) −0.004658* Growth phase^2 −1.60629* Concentration of Buffer^2 + 0.006969 (Growth phase^2 * Concentration of Buffer) + 0.604500 (Concentration of Buffer^2 * Number of cycles) (Fig. 5, Fig. 6, Fig. 7).

3.2. FTIR analysis of extracted phycocyanin

The FTIR spectrum of the extracted phycocyanin displayed transmittance maxima at 1649 cm^{-1}, as shown in Fig. 8. This is consistent with the findings of Al-Malki (2020), wherein the maximum transmittance of Phycocyanin was 1652 cm^{-1}.

3.3. SDS PAGE of extracted Phycocyanin

The two distinct protein bands with molecular weights between > 15 and < 25 kD likely correspond to pure Phycocyanin (Fig. 9). Both α and β subunits form the core structure of the protein and are present in equal numbers (Cai et al., 2001).

3.4. GCMS analysis of Phycocyanin

The GC–MS analysis of Phycocyanin revealed significant peaks at 21.10 min and 26.56 min (Fig. 10). To confirm the presence of phycocyanin, a comparison with a standard and referencing Al-Malki's findings in 2020 was conducted, leading to a conclusive identification of phycocyanin in the extract.

Additionally, the chromatogram's five peaks were cross-referenced with library databases, and the results have been compiled into a cumulative table for further analysis [Table 4].

3.5. Antioxidant potential of Phycocyanin

Spirulina is recognized for its potent antioxidant properties, and these attributes are mainly due to the presence of phycobiliproteins within it. Among the phycobiliproteins, phycocyanin is the predominant component in Spirulina (Martelli et al., 2014). In our study, we conducted a series of diverse antioxidant assays to evaluate and quantify the antioxidant potential of Phycocyanin extracted from *Spirulina platensis* PCC 7345, as illustrated in Fig. 11.

From the Graph (Fig. 11), the following data has been derived (Table 5).

The IC50 values represent the concentration of phycocyanin at which it achieves 50% inhibition in various antioxidant assays. Specifically, in the DPPH, ABTS, and NO Radical scavenging assays, the IC50 values for

phycocyanin were determined to be 40.70 μg/ml, 23.25 μg/ml, and 17.74 μg/ml, respectively.

3.6. Enzyme inhibitory assays

3.6.1. Inhibition of α-Amylase enzyme

Both α-Amylase and α-Glucosidase enzymes are pivotal in carbohydrate metabolism, and elevated levels of these enzymes are commonly observed in hyperglycemic patients. Inhibiting these enzymes is a fundamental strategy for preventing glycation and its associated complications, such as diabetes and obesity [Gong et al., 2020; Payan, 2004].

Fig. 12a presents the findings of the α-Amylase inhibitory assay, demonstrating the potent inhibitory effect of phycocyanin on α-amylase across various concentrations. The highest level of inhibition (61.47%) was achieved at a concentration of 100 μg/ml, with an approximate IC50 value of 72.24 μg/ml (Table 5). This underscores the concentration-dependent inhibitory capacity of phycocyanin on α-amylase.

3.6.2. Inhibition of α-Glucosidase enzyme

Fig. 12b presents the results of the α-Glucosidase inhibition assay, demonstrating the potent inhibitory effect of phycocyanin on α-Glucosidase across various concentrations. The highest level of inhibition (76.54%) was achieved at a concentration of 100 μg/ml, with an approximate IC50 value of 82.45 μg/ml (Table 6). This underscores the concentration-dependent inhibitory capacity of phycocyanin on α-Glucosidase.

4. Discussion

The adoption of a Quality by Design (QbD) framework in this study involved a meticulous review of the literature to define Target Product Profiles (TPPs) and Critical Quality Attributes (CQAs) (Dhoble and Patravale, 2019). The chosen CQAs, Phycocyanin concentration, and purity were selected due to their direct influence on the quality and efficacy of the final Phycocyanin product. The risk assessment phase unveiled factors with notable impacts on Phycocyanin concentration and purity. Ishikawa diagrams (cause and effect diagrams) were instrumental in identifying influential variables (Aoki et al., 2021; Asayama, 2012; Kuddus et al., 2013; Kumar et al., 2014; Seo et al., 2013; Wang et al., 2001). Notably, the concentration of the extraction buffer, the growth phase of the culture, and the number of freeze–thaw cycles emerged as key contributors to these critical attributes. The Box Behnken design, employed for its systematic evaluation of factors, facilitated the exploration of Phycocyanin concentration and purity across a broad spectrum. The results exhibited variations within the matrix of 15 formulations, ranging from 0.0121 to 0.2812 mg/ml for concentration and 0.17 to 0.6978 for purity.

The FTIR analysis corroborated the quality and consistency of the extracted Phycocyanin. Notably, a transmittance maximum at 1649 cm^{-1} was consistent with previous findings, reinforcing the reliability of the Phycocyanin product. Al-Malki (2020) extracted phycocyanin from *Ulva lactuca* algae and reported the maximum transmittance of phycocyanin as 1652 cm^{-1}. A similar FTIR spectrum was observed by Husain et al. (2022), where phycocyanin was extracted from *Plectonema* sp. The FTIR spectrum of the analyzed sample, as depicted in Fig. 8, reveals four prominent peaks, each associated with specific functional groups or molecular vibrations inherent to phycocyanin. The signal observed at approximately 1649 cm^{-1} is indicative of the amide I band, a characteristic feature of proteins like phycocyanin. This band primarily arises from the stretching vibrations of the carbonyl (C = O) group within the peptide bonds of the protein structure (Sadat and Joye, 2020).

Furthermore, the signal at 1587 cm^{-1} aligns with the amide II band and/or aromatic rings present in proteins, emphasizing the proteinaceous nature of phycocyanin (Hernández et al., 2010). Symmetric bending vibrations of methyl groups is associated with the signal around 1398 cm^{-1} (Hannah and Mayo, 2004). Additionally, the FTIR signal at 1115 cm^{-1} is consistent with C-O stretching vibrations in ethers or esters, providing insights into specific chemical bonds within the phycocyanin molecular structure. This signal may also correspond to C–C stretching vibrations in alkanes, adding to the comprehensive characterization of phycocyanin's chemical composition (Liu and Kim, 2017).

The SDS-PAGE analysis revealed two distinct protein bands with molecular weights between $>$ 15 and $<$ 25 kD, indicative of pure Phycocyanin. This observation aligns with the findings reported by Santiago-Santos et al. (2004), where similar SDS-PAGE bands of Phycocyanin extracted from *Calothrix* sp. were characterized with molecular weights of approximately 17 kD and 21 kD, respectively. This alignment with established literature further validated the structural integrity of the protein core composed of both α and β subunits.

The GC spectrum displayed noticeable peaks at 21.10 min and 26.56 min. Through meticulous scrutiny and comparison with the standard, and in concordance with the findings of Al-Malki's research in 2020, it was evident that analogous peaks were observed. Notably, Qian and colleagues (2023) reported similar peak observations with commercial phycocyanin. This comprehensive analysis confirmed the presence of phycocyanin in the extract.

An array of diverse antioxidant assays underscored the robust antioxidant potential of Phycocyanin. The calculated IC50 values, representing the concentration at which 50% inhibition occurs in these assays, provided empirical evidence of Phycocyanin's superior antioxidant capacity compared to *Spirulina platensis* PCC 7345 aqueous extract. Comparing these findings to our prior research on the antioxidant potential of *Spirulina platensis* PCC 7345 aqueous extract (as documented in Paramanya et al., 2023a), it becomes evident that phycocyanin exhibits significantly higher antioxidant potential than the extract itself. This observation suggests that phycocyanin may play a pivotal role as one of the key factors contributing to Spirulina's overall antioxidant properties. A consistent rise in antioxidant potential in a concentration-dependent manner was observed in both ABTS and DPPH assays, aligning with the findings reported by Wu et al. 2016.

Our findings suggest that phycocyanin has the potential to regulate α-amylase and α-glucosidase activity, a significant enzyme in carbohydrate digestion. Similar concentration-dependent inhibition of these enzymes by phycocyanin has been reported by Prabakaran et al. (2020), where phycocyanin showed a dose-dependent and maximum inhibition effect at 250 μg/ml. This inhibition may have implications for conditions like obesity and diabetes, where carbohydrate metabolism plays a crucial role. Balyan et al. (2023) have reported a direct correlation between the inhibition of these enzymes and the antiglycation potential of their samples. Subsequent phases of our research will focus on elucidating the antiglycation potential of the extracted Phycocyanin.

5. Conclusions

Quality by Design (QbD) serves as a systematic framework for optimizing the phycocyanin extraction process, ensuring heightened control and predictability concerning concentration and purity outcomes. Employing Ishikawa diagrams and Box-Behnken design, the investigation discerned crucial factors influencing phycocyanin extraction, facilitating risk mitigation and comprehensive exploration. Robust analytical techniques confirmed the consistency and structural integrity of the extracted phycocyanin. The discerned antioxidant properties and concentration-dependent inhibition of carbohydrate-metabolism enzymes position phycocyanin as a promising candidate for diverse applications. This research contributes a refined extraction methodology and paves the way for further scientific inquiries into the health, wellness, and industrial utility of phycocyanin.

Funding

Researchers Supporting Project Number (RSPD2023R710) from King Saud University, Riyadh, Saudi Arabia.

Institutional Review Board Statement
Not applicable.
Informed Consent Statement
Not applicable.

CRediT authorship contribution statement

Additiya Paramanya: Methodology, Software, Validation, Formal analysis, Investigation, Data curation, Writing – original draft, Visualization. **Abeeb Oyesiji Abiodun:** Conceptualization, Methodology, Validation, Resources, Writing – review & editing, Funding acquisition. **Mohammad Shamsul Ola:** Validation, Resources, Writing – review & editing, Funding acquisition. **Ahmad Ali:** Validation, Resources, Data curation, Visualization, Supervision, Project administration.

Declaration of Competing Interest

The authors declare that they have no known competing financial interests or personal relationships that could have appeared to influence the work reported in this paper.

Acknowledgement

The authors thank the Sophisticated Analytical Instrumental Facility (SAIF) at IIT Bombay for providing instrumentation for FTIR and GC Analysis. The author thanks Dr. Dhoble from the Institute of Chemical Technology (ICT), Mumbai, India, for helping to understand RSM. The authors would also like to thank the funding support from Researchers Supporting Project Number (RSPD2024R710), King Saud University, Riyadh, Saudi Arabia.

References

Al-Malki, A., 2020. In vitro cytotoxicity and pro-apoptotic activity of phycocyanin nanoparticles from Ulva lactuca (Chlorophyta) algae. Saudi J. Bio. Sci. 27 (2020), 894–898.
Aoki, J., Sasaki, D., Asayama, M., 2021. Development of a method for phycocyanin recovery from filamentous cyanobacteria and evaluation of its stability and antioxidant capacity. BMC Biotechnol. 21 (1), 40. https://doi.org/10.1186/s12896-021-00692-9.
Asayama, M., 2012. Overproduction and easy recovery of target gene products from cyanobacteria, photosynthesizing microorganisms. Appl. Microbiol. Biotechnol. 95 (3), 683–695. https://doi.org/10.1007/s00253-012-3989-0.
Balyan, P., Ali, A., 2022. Comparative analysis of the biological activities of different extracts of *Nigella sativa* L. seeds. Ann. Phytomedicine Int. J. 11, 577–587.
Balyan, P., Ola, M.S., Alhomida, A.S., Ali, A., 2022. D-Ribose-Induced Glycation and Its Attenuation by the Aqueous Extract of *Nigella sativa* Seeds. Medicina (Kaunas). 58 (12), 1816. https://doi.org/10.3390/medicina58121816.
Bennett, A., Bogorad, L., 1973. Complementary Chromatic Adaptation in a Filamentous Blue-Green Alga. J. Cell. Biol. 58, 419–435. https://doi.org/10.1083/jcb.58.2.419.
Betz, J.M., Brown, P.N., Roman, M.C., 2011. Accuracy, precision, and reliability of chemical measurements in natural products research. Fitoterapia 82 (1), 44–52. https://doi.org/10.1016/j.fitote.2010.09.011.
Cai, Y.A., Murphy, J.T., Wedemayer, G.J., Glazer, A.N., 2001. Recombinant phycobiliproteins: recombinant C-phycocyanins equipped with affinity tags, oligomerization, and biospecific recognition domains. Anal. biochem. 290 (2), 186–204.
Chirumamilla, P., Dharavath, S.B., Taduri, S., 2022. GC-MS profiling and antibacterial activity of Solanum khasianum leaf and root extracts. Bull. Natl. Res. Cent. 46 (1), 127. https://doi.org/10.1186/s42269-022-00818-9.
Dhoble, S., Patravale, V., 2019. Development of anti-angiogenic erlotinib liposomal formulation for pulmonary hypertension: a QbD approach. Drug. Deliv. Transl. Res. 9 (5), 980–996. https://doi.org/10.1007/s13346-019-00641-2.
Fernandes, R., Campos, J., Serra, M., 2023. Exploring the Benefits of Phycocyanin: From Spirulina Cultivation to Its Widespread Applications. Pharmaceuticals (Basel). 16 (4), 592. https://doi.org/10.3390/ph16040592.
Gong, L., Feng, D., Wang, T., Ren, Y., Liu, Y., Wang, J., 2020. Inhibitors of α-amylase and α-glucosidase: Potential linkage for whole cereal foods on prevention of hyperglycemia. Food Sci. Nutr. 8 (12), 6320–6337. https://doi.org/10.1002/fsn3.1987.
Hannah, R.W., Mayo, D.W. 2004. Course Notes on the Interpretation of Infrared and Raman Spectra. In book: Course Notes on the Interpretation of Infrared and Raman Spectra. DOI: 10.1002/0471690082.answ.
Hernández, B., Pflüger, F., Adenier, A., Kruglik, S.G., Ghomi, M., 2010. Vibrational Analysis of Amino Acids and Short Peptides in Hydrated Media. VIII. Amino Acids with Aromatic Side Chains: Phenylalanine, Tyrosine, and Tryptophan. J. Phy. Chem. B. 114 (46), 15319–15330. https://doi.org/10.1021/jp106786j.
Husain, A., Farooqui, A., Khanam, A., 2022. Physicochemical characterization of C-phycocyanin from Plectonema sp. and elucidation of its bioactive potential through in silico approach. Cell Mol. Biol. (Noisy-le-grand) 67 (4), 68–82. https://doi.org/10.14715/cmb/2021.67.4.8.
Kazeem, M.I., Adamson, J.O., Ogunwande, I.A., 2013. Modes of Inhibition of α-Amylase and α-Glucosidase by Aqueous Extract of *Morinda Lucida* Benth Leaf. Bio. Med. Res. Int. 2013, 1–6. https://doi.org/10.1155/2013/527570.
Kuddus, M., Singh, P., Thomas, G., Awdah, A-H. 2013. Recent developments in production and biotechnological applications of C-phycocyanin. Biomed. Res. Int. pp. 742859:1–9. doi: 10.1155/2013/742859.
Kumar, D., Ali, A., 2019. Antiglycation and Antiaggregation Potential of Thymoquinone. Nat. Volatiles Essent. Oils. 6, 25–33.
Kumar, D., Dhar, D.W., Pabbi, S., Kumar, N., Walia, S., 2014. Extraction and purification of C-phycocyanin from Spirulina platensis (CCC540) Ind. J. Plant Physiol. 19 (2), 184–188. https://doi.org/10.1007/s40502-014-0094-7.
Li, Y., Zhang, Z., Paciulli, M., Abbaspourrad, A., 2020. Extraction of phycocyanin-A natural blue colorant from dried spirulina biomass: Influence of processing parameters and extraction techniques. J. Food Sci. 85 (3), 727–735. https://doi.org/10.1111/1750-3841.14842.
Liu, Y., Kim, H.Y., 2017. Fourier Transform Infrared Spectroscopy (FT-IR) and Simple Algorithm Analysis for Rapid and Non-Destructive Assessment of Developmental Cotton Fibers. Sensors. 17 (7), 1469. https://doi.org/10.3390/s17071469.
López, R., Fernández, C., Pereira, F.J., Díez, A., Cara, J., Martínez, O., Sánchez, M.E., 2020. A Comparison between Several Response Surface Methodology Designs and a Neural Network Model to Optimise the Oxidation Conditions of a Lignocellulosic Blend. Biomolecules. 10 (5), 787. https://doi.org/10.3390/biom10050787.
Martelli, G., Folli, C., Visai, L., Daglia, M., Ferrari, D., 2014. Thermal stability improvement of blue colorant C-phycocyanin from Spirulina platensis for food industry applications. Process Biochem. 49 (1), 154–159. https://doi.org/10.1016/j.procbio.2013.10.008.
Martinez-Gonzalez, AI., Díaz-Sánchez, Á,G., Rosa, L.A., Vargas-Requena, C.L., Bustos-Jaimes, I., Alvarez-Parrilla, A.E. 2017. Polyphenolic Compounds and Digestive Enzymes: In Vitro Non-Covalent Interactions. Molecules. 22(4), pp. 669. doi: 10.3390/molecules22040669.
Pagels, F., Guedes, A.C., Amaro, H.M., Kijjoa, A., Vasconcelos, V., 2019. Phycobiliproteins from cyanobacteria: Chemistry and biotechnological applications. Biotech. Adv. 37 (3), 422–443. https://doi.org/10.1016/j.biotechadv.2019.02.010.
Paramanya, A., Ali, A., 2019. Role of Oxidative Stress in Biological Systems. Middle East J. Sci. 5 (2), 155–162. https://doi.org/10.23884/mejs.2019.5.2.07.
Paramanya, A., Farah, M.A., Al-Anazi, K.M., Devkota, H.P., Ali, A., 2023a. Exploring the Potential of Spirulina (Arthrospira platensis) Aqueous Extract in Preventing Glycation of Hemoglobin and pBR322 Plasmid. Pharmacogn. Mag. 19 (3), 581–591. https://doi.org/10.1177/09731296231170959.
Paramanya, A., Siddiqui, S.A., Poojari, P., Jamkhedkar, S., Khan, J., Almeida, J.R.G.S., Ali, A., 2023b. Ethnic Knowledge on Biodiversity, Nutrition, and Health Security, Vol 1. Apple Academic Press. https://doi.org/10.1201/9781003353089-12.
Payan, F., 2004. Structural basis for the inhibition of mammalian and insect alpha-amylases by plant protein inhibitors. Biochim. Biophys. Acta. 1696 (2), 171–180. https://doi.org/10.1016/j.bbapap.2003.10.012.
Pokhrel, T., Shrestha, D., Dhakal, K., Yadav, P.M., Adhikari, A. 2022. Comparative analysis of the antioxidant and antidiabetic potential of *Nelumbo nucifera Gaertn.* and *Nymphaea lotus* L. var. pubes1. J. Chem. doi:10.1155/2022/4258124..
Poojari, P., Paramanya, A., Padgaonkar, A., Ali, A., 2022. Compendium Of Polycystic Ovarian Syndrome And Its Relevance In Glycation And Diabetes. J. Exp. Clin. Med. 39 (1), 256–268. https://doi.org/10.52142/omujecm.39.1.49.
Prabakaran, G., Sampathkumar, P., Kavisri, M., Moovendhan, M., 2020. Extraction and characterization of phycocyanin from *Spirulina platensis* and evaluation of its anticancer, antidiabetic and antiinflammatory effect. Int. J. Biol. Macromol. 153, 256–263. https://doi.org/10.1016/j.ijbiomac.2020.03.009.
Qian, L., Ni, J., Xu, W., Yuan, C., Wang, S., Hu, Y., Gu, H., 2023. Phycocyanin to biocrude via the integration of isothermal/fast hydrothermal liquefaction and aqueous phase recirculation: Reaction products and process analyses. Fuel 332, 126226.
Sadat, A., Joye, I.J., 2020. Peak Fitting Applied to Fourier Transform Infrared and Raman Spectroscopic Analysis of Proteins. App. Sci. MDPI AG. 10 (17), 5918. https://doi.org/10.3390/app10175918.
Santiago-Santos, Ma.C, Ponce-Noyola, T., Olivera-Ramirez, R., Ortega-Lopez, J., Canizares-Villanueva, R.O. 2004. Extraction and purification of phycocyanin from *Calothrix* sp. Proc. Biochem. 39, pp. 2047–2052.
Sathiavelu, A., Sangeetha, S., Archit, R., Mythili, S., 2013. In Vitro Anti-Diabetic Activity of Aqueous Extract of the Medicinal Plants *Nigella Sativa, Eugenia Jambolana, Andrographis Paniculata* and *Gymnema Sylvestre*. Int. J. Drug Dev. Res. 5, 323–328.
Seo, Y.C., Choi, W.S., Park, J.H., Park, J.O., Jung, K,H., Lee, H.Y. 2013. Stable isolation of phycocyanin from *Spirulina platensis* associated with high-pressure extraction process. Int. J. Mol. Sci. 14(1), pp. 1778–1787. doi: 10.3390/ijms14011778.
Shrestha, D., Sharma, P., Adhikari, A., Mandal, A.K., Verma, A., 2021. A review on Nepalese medicinal plants used traditionally as alpha-amylase and alpha-glucosidase inhibitors against diabetes mellitus. Curr. Trad. Med. 7 (5), 1.
Silveira, S.T., Burkert, J.F., Costa, J.A., Burkert, C.A., Kalil, S.J., 2007. Optimization of phycocyanin extraction from Spirulina platensis using factorial design. Biores. Tech. 98 (8), 1629–1634. https://doi.org/10.1016/j.biortech.2006.05.050.
Tan, H.T., Khong, N.M.H., Khaw, Y.S., Ahmad, S.A., Yusoff, F.M., 2020. Optimization of the Freezing-Thawing Method for Extracting Phycobiliproteins from *Arthrospira* sp. Molecules. 25 (17), 3894. https://doi.org/10.3390/molecules25173894.

Wang, X.Q., Li, L.N., Chang, W.R., Zhang, J.P., Gui, L.L., Guo, B.J., Liang, D.C., 2001. Structure of C-phycocyanin from Spirulina platensis at 2.2 Å resolution: a novel monoclinic crystal form for phycobiliproteins in phycobilisomes. Acta. Crystallogr. Sect. D. Biol. Crystallogr. 57 (6), 784–792. https://doi.org/10.1107/S0907444901004528.

Wu, H.L., Wang, G.H., Xiang, W.Z., Li, T., He, H., 2016. Stability and antioxidant activity of food-grade phycocyanin isolated from Spirulina platensis. Int. J. Food Prop. 19 (10), 2349–2362. https://doi.org/10.1080/10942912.2015.1038564.

Yu, L., Amidon, G., Khan, M.A., Hoag, S.W., Polli, J., Raju, G.K., Woodcock, J., 2014. Understanding pharmaceutical quality by design. The AAPS J. 16 (4), 771–783. https://doi.org/10.1208/s12248-014-9598-3.